Experiment 4B: The rotational-vibrational spectrum of HCl

Sam White (Author) and Emma Winful (Laboratory Partner)

30/11/2018

Abstract

The rotational constants, $\tilde{B}_\nu$, were determined for both common isotopologues of HCl gas and hence the bond force constants, k. The rotational constants for $H^{35}Cl$ were in agreement with published values and the bond force constants found were $477.383 \pm 0.001\,\mathrm{N\,m^{-1}}$ and $480.698 \pm 0.006\,\mathrm{N\,m^{-1}}$ for $H^{35}Cl$ and $H^{37}Cl$ respectively. The bond force constants are not identical within reasonable errors, hence it is likely that the isotopic mass affects the value of k, however additional data should be collected to verify this.

1 Results and Analysis

1.1 Collected Data

Table 1: Rotational-vibrational absorbance wavelengths for the fundamental transition bands.

	J	$R(J)$ / $\mathrm{cm^{-1}}$	$P(J)$ / $\mathrm{cm^{-1}}$	$R(J)-P(J)$ / $\mathrm{cm^{-1}}$	$R(J-1)-P(J+1)$ / $\mathrm{cm^{-1}}$
$H^{35}Cl$	0	2906.4			
	1	2926.03	2865.24	60.79	62.64
	2	2945.05	2843.76	101.29	104.33
	3	2963.42	2821.70	141.72	145.98
	4	2981.14	2799.07	182.07	187.53
	5	2998.19	2775.89	222.30	228.97
	6	3014.57	2752.17	262.40	270.26
	7	3030.27	2727.93	302.34	311.4
	8	3045.28	2703.17	342.11	352.37
	9	3059.52	2677.90	381.62	393.13
	10	3073.10	2652.15	420.95	433.62
	11	3085.88	2625.90	459.98	473.88
	12		2599.22		
$H^{37}Cl$	0	2904.29			
	1	2923.91	2863.20	60.71	62.53
	2	2942.90	2841.76	101.14	104.19
	3	2961.24	2819.72	141.52	145.76
	4	2978.93	2797.14	181.79	187.25
	5	2995.96	2773.99	221.97	228.62
	6	3012.32	2750.31	262.01	269.86
	7	3027.98	2726.10	301.88	310.95
	8	3042.97	2701.37	341.60	351.84
	9	3057.22	2676.14	381.08	392.57
	10	3070.73	2650.40	420.33	432.99
	11	3083.51	2624.23	459.28	473.20
	12		2597.53		

Table 2: Rotational-vibrational absorbance wavelengths for the overtone transition bands.

	J	$R(J)$ / cm^{-1}	$P(J)$ / cm^{-1}	$R(J) - P(J)$ / cm^{-1}	$R(J-1) - P(J+1)$ / cm^{-1}
$H^{35}Cl$	0	5688.16			
	1	5706.59	5647.71	58.88	62.66
	2	5723.78	5625.50	98.28	104.35
	3	5739.75	5602.24	137.51	145.98
	4	5754.53	5577.80	176.73	187.53
	5	5767.89	5552.22	215.67	229.05
	6	5780.07	5525.48	254.59	270.26
	7	5790.92	5497.63	293.29	311.52
	8		5468.55		
$H^{37}Cl$	0	5684.12			
	1	5703.13	5643.60	59.53	62.58
	2	5719.67	5621.54	98.13	104.80
	3	5735.61	5598.33	137.28	145.76
	4	5750.30	5573.91	176.39	197.19
	5	5763.27	5548.42	214.85	228.64
	6	5775.12	5521.66	253.46	269.43
	7	5786.65	5493.84	292.81	310.49
	8		5464.63		

1.2 Determination of Rotational Constants and Bond Lengths

The values of the rotational constants $\tilde{B}_0$, $\tilde{B}_1$ and $\tilde{B}_2$ were calculated accounting for the centrifugal distortion of the molecules by plotting graphs of $\frac{R(J)-P(J)}{J+\frac{1}{2}}$ and $\frac{R(J-1)-P(J+1)}{J+\frac{1}{2}}$ against $(J+\frac{1}{2})^2$ and performing linear regressions (as shown in figures 1 and 2). This was completed since if combination differences between the $R(J)$ and $P(J)$ and then the $R(J-1)$ and $P(J+1)$ bands are taken and the centrifugal distortion accounted for the resultant equations can be re-arranged to give equations 1.2.1 and 1.2.2 respectively, where $\tilde{D}_\nu$ are the centrifugal distortion coefficients. These equations are in the form of the general equation of a straight line, $y = mx + c$, hence the plotted data can be fitted by a function of this form.

$$\frac{R(J) - P(J)}{J + \frac{1}{2}} = -8\tilde{D}_1 \left(J + \frac{1}{2}\right)^2 + 4\tilde{B}_1 - 6\tilde{D}_1 \tag{1.2.1}$$

$$\frac{R(J-1) - P(J+1)}{J + \frac{1}{2}} = -8\tilde{D}_0 \left(J + \frac{1}{2}\right)^2 + 4\tilde{B}_0 - 6\tilde{D}_0 \tag{1.2.2}$$

The values of $\tilde{D}_\nu$ were then determined (see table 6 in the supplementary information) and hence the rotational constants, $\tilde{B}_\nu$, shown in table 3 were calculated. The error propagation shown in equation 1.2.3 was then completed to estimate the uncertainties in $\tilde{B}_\nu$, where $\alpha_{\tilde{B}_\nu}$, α_m and α_c are the uncertainties in $\tilde{B}_\nu$, the gradient of the fitted line and the intercept respectively.

$$\alpha_{\tilde{B}_\nu} = \sqrt{\left(\frac{3}{16}\alpha_m\right)^2 + \left(\frac{1}{4}\alpha_c\right)^2} \tag{1.2.3}$$

The literature values of $\tilde{B}_\nu$ for $H^{35}Cl$, $\tilde{B}_{\nu_{Lit.}}$, in table 3 were determined using published equilibrium rotational constant, $\tilde{B}_e$, and rotational constant parameter, α_e, values[1] with equation 1.2.4.

$$\tilde{B}_{\nu_{Lit.}} = \tilde{B}_e - \alpha_e \left(\nu + \frac{1}{2}\right) \tag{1.2.4}$$

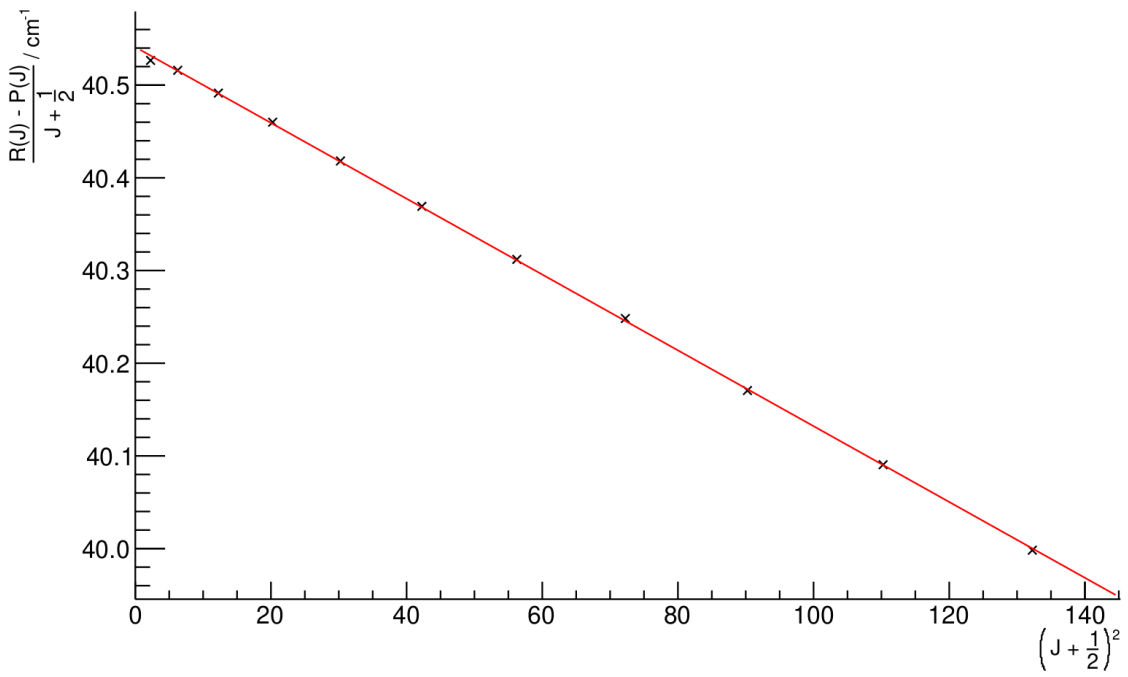

Figure 1: Graph showing the linear regression performed for the upper rotational (R) branch of the fundamental transition in $H^{35}Cl$.

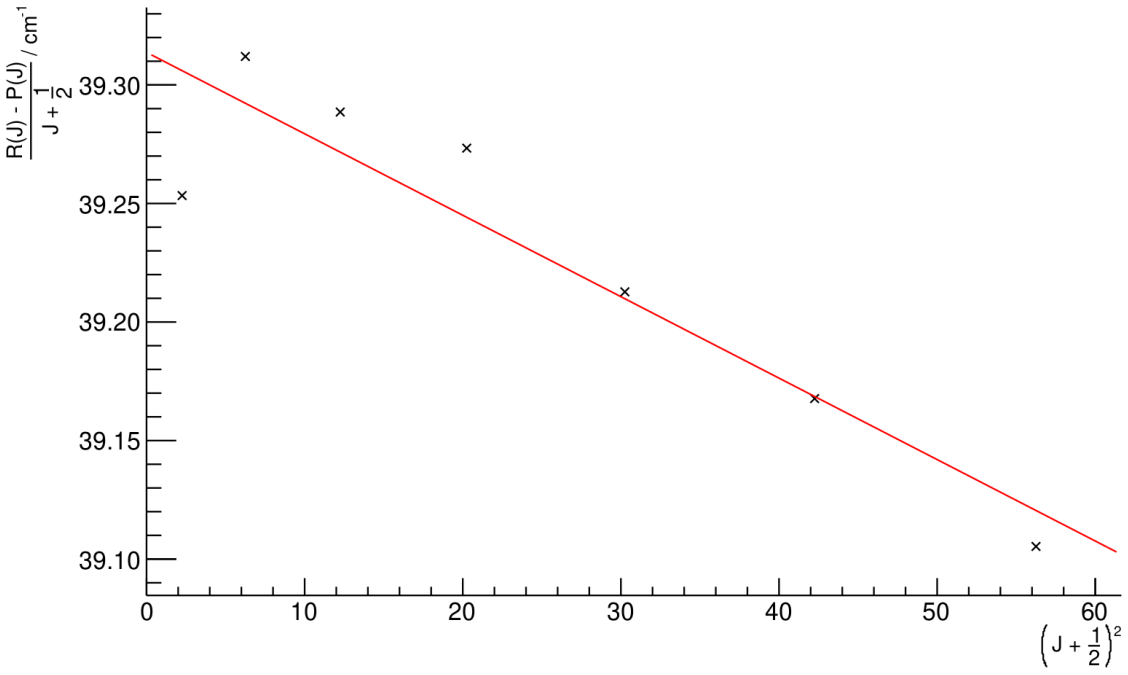

Figure 2: Graph showing the linear regression performed for the upper rotational (R) branch for the overtone transition in $H^{35}Cl$.

The bond lengths in table 3 were determined from the $\tilde{B_\nu}$ values using equation 1.2.5. Furthermore the calculus-based approximation[2] was utilised to propagate the uncertainties in $\tilde{B_\nu}$ for r_ν (α_{r_ν}) as the $\alpha_{\tilde{B_\nu}}$ values are small hence producing equation 1.2.6. The uncertainties in the values of the constants and reduced mass used[3] are insignificant compared to that of $\alpha_{\tilde{B_\nu}}$, and hence they were excluded from the error propagation.

$$r_\nu = \sqrt{\frac{h}{8\pi^2 c\mu\tilde{B}_\nu}} \tag{1.2.5}$$

$$\alpha_{r_\nu} = \frac{1}{2}\sqrt{\frac{h}{8\pi^2 c\mu\tilde{B}_\nu{}^3}}\alpha_{\tilde{B}_\nu} \tag{1.2.6}$$

Table 3: Rotational constants and bond lengths.

	ν	$\tilde{B}_\nu$ / cm^{-1}	$\tilde{B}_{\nu_{Lit.}}$ / cm^{-1}	r_ν / pm
$H^{35}Cl$	0	10.4408 ± 0.0004	10.439 82	128.823 ± 0.002
	1	10.1360 ± 0.0002	10.132 64	130.745 ± 0.001
	2	9.829 ± 0.004	9.825 46	132.77 ± 0.02
$H^{37}Cl$	0	10.4248 ± 0.0003		128.385 ± 0.002
	1	10.1214 ± 0.0001		130.2953 ± 0.0009
	2	9.86 ± 0.02		132.0 ± 0.1

1.3 Determination of Vibrational Constants

The harmonic constant, $\tilde{\nu_e}$, and the anharmonicity constant, x_e, in table 4 were determined using equations 1.3.1 and 1.3.2. The derivation method of these equations is included in section 3.2 within the supplementary information.

$$\tilde{\nu_e} = R(0) - 3\tilde{B}_1 + \tilde{B}_2 \tag{1.3.1}$$

$$x_e = \frac{1}{2}\frac{\tilde{B}_2 - \tilde{B}_1}{R(0) - 3\tilde{B}_1 + \tilde{B}_2} \tag{1.3.2}$$

The uncertainties in these values was estimated using equations 1.3.3 and 1.3.4 with the uncertainty in $R(0)$ excluded from the propagation as it is negligible compared to that in $\tilde{B}_1$ and $\tilde{B}_2$ since it is determined by reading the absorption wavenumber directly from the spectrum.

$$\alpha_{\tilde{\nu_e}} = \sqrt{\left(3\alpha_{\tilde{B}_1}\right)^2 + \left(\alpha_{\tilde{B}_2}\right)^2} \tag{1.3.3}$$

$$\alpha_{x_e} = x_e\sqrt{\frac{\left(\alpha_{\tilde{B}_1}\right)^2 + \left(\alpha_{\tilde{B}_2}\right)^2}{\left(\tilde{B}_2 - \tilde{B}_1\right)^2} + \left(\frac{\alpha_{\tilde{\nu_e}}}{\tilde{\nu_e}}\right)^2} \tag{1.3.4}$$

Table 4: Vibrational Coefficients.

	$H^{35}Cl$	$H^{37}Cl$
$\tilde{\nu_e}$ / cm^{-1}	2885.821 ± 0.004	2883.78 ± 0.02
x_e / 10^{-5}	-5.32 ± 0.06	-4.5 ± 0.3

1.4 Determination of Bond Force Constants

The bond force constants, k, in table 5 were determined using equation 1.4.1 and the error in k, α_k, was determined using equation 1.4.2 (derived using the calculus-based approximation). The errors in μ and the constants were again not considered as they are negligible compared to that of ν_e.

$$k = 4\pi^2 c^2 \mu\tilde{\nu_e}^2 \tag{1.4.1}$$

$$\alpha_k = 8\pi^2 c^2 \mu\tilde{\nu_e}\alpha_{\tilde{\nu_e}} = 8\pi^2 c^2 \mu\tilde{\nu_e}\sqrt{\left(3\alpha_{\tilde{B}_1}\right)^2 + \left(\alpha_{\tilde{B}_2}\right)^2} \tag{1.4.2}$$

Table 5: Force Constants.

	$H^{35}Cl$	$H^{37}Cl$
k / $N\,m^{-1}$	477.383 ± 0.001	480.698 ± 0.006

2 Discussion

2.1 Errors and Analysis Method

It is likely that the errors used for the data collected are underestimates since they are derived from linear regressions performed with a limited number of data points (less than 12). Furthermore while the linear regression was (in general) good for the data obtained for fundamental transitions ($2 \times 10^{-5} < \chi^2 < 2 \times 10^{-4}$) it was much poorer for data derived from the overtone transition ($4 \times 10^{-4} < \chi^2 < 0.2$). This was due to the considerable signal:noise ratio on the spectrum for the overtone transition resulting in the data being significantly affected by random noise (as can be seen in figure 2) and hence the true uncertainty in these values is likely to be even greater.

The high signal:noise ratio for the overtone transition data is due to the low overtone transition probability since the transition is forbidden by the $\Delta\nu = \pm 1$ selection rule obtained for the purely harmonic potential and while the oscillator is anharmonic it still has considerable harmonic character. The signal:noise ratio could be reduced by recording additional spectra for just the overtone region (6000–5000 cm^{-1}) with a greater concentration of HCl in the gas cell. The reduced wavenumber range should be used since the increased concentration will also increase the intensity of the fundamental transition peaks and will cause them to be 'cut' hence preventing a distinct wavenumber from being recorded for the fundamental transition absorption peak. In addition to this further spectra for the fundamental transition could be recorded as well to allow a better estimation of the errors in these values by aiding in determining the reproducibility of the results.

Corrections were made in the data analysis for centrifugal distortion since when the effect of this was ignored the residuals for the resultant regression followed a distinctive parabolic-like pattern when plotted opposed to being randomly distributed, thus indicating the presence of a systematic error. When the centrifugal distortion was considered the residuals instead appeared to be much more randomly distributed.

2.2 Data

2.2.1 Rotational Constants

The $\tilde{B}_0$ values tabulated in table 3 were derived using data from the fundamental transition only even though they could have also been determined using data from the overtone transition. This method was used due to the large random errors in the overtone transition data (due to the high signal:noise ratio as discussed in section 2.1), so any use of the data from this would be likely to greatly increase the random errors associated with the $\tilde{B}_0$ value.

From equation 2.2.1 it was expected that $\tilde{B}_\nu$ for $H^{35}Cl$ should be larger than the corresponding values for $H^{37}Cl$ due to the larger reduced mass of $H^{37}Cl$.

$$\tilde{B}_\nu = \frac{h}{8\pi^2 c\mu r^2} \tag{2.2.1}$$

The data in table 3 agrees with this as almost all values of $\tilde{B}_\nu$ stated for $H^{35}Cl$ are larger than the corresponding values for $H^{37}Cl$ except for the $\tilde{B}_2$ value. However using the uncertainty in the $\tilde{B}_2$ value for $H^{37}Cl$ there is a probability of 6.06 % that the true value actually satisfies this condition (calculated by assuming the measurements are normally distributed around the true value). In fact since the uncertainties estimated are likely underestimates (see section 2.1) this probability will be higher in reality, hence it is probable that the data agrees with the expectation drawn from equation 2.2.1. To increase the certainty of this statement more spectra should be obtained for the overtone transition with a lower signal:noise ratio and hence smaller random error (as discussed in section 2.1).

The values of $\tilde{B}_\nu$ in table 3 all agree with the literature values, $\tilde{B}_{\nu_{Lit.}}$, within $\pm 0.004\,\mathrm{cm}^{-1}$. While this is one order of magnitude greater than the estimated uncertainties in all values (except for $\tilde{B}_2$) it is likely that the obtained data does agree with these literature values (as discussed in section 2.1) as the uncertainties stated are likely underestimates.

2.2.2 Bond Lengths

It was expected that the bond lengths, r_ν, of both isotopologues would increase as ν increased since the asymmetry of the anharmonic bond potential should cause the mean bond length to increase with the vibrational energy level. All of the values of r_ν obtained in table 3 show this trend.

In table 3 it can also be seen that the bond lengths of the $H^{37}Cl$ isotopologue in each vibrational state are greater than those for the $H^{35}Cl$ isotopologue. This can be justified theoretically using the one dimensional Schödinger equation (equation 2.2.2) where for a (stationary) state described by ψ_ν in a constant potential $V(x)$ increasing the reduced mass, μ, should reduce the energy of the state, E_ν, hence reducing the mean bond length due to the anharmonicity of the potential.

$$\begin{aligned} E_\nu \psi_\nu &= \hat{H}\psi_\nu \\ &= \left(\frac{\hat{p}^2}{2\mu} + V(x)\right)\psi_\nu \end{aligned} \tag{2.2.2}$$

2.2.3 Bond Force Constants

It was expected that the bond force constants, k, displayed in table 5 should be equal for both isotopologues as it was assumed that k depends only on the chemical bonding and hence should be the same.

Despite this the force constants differ by $3.315\,\mathrm{N\,m}^{-1}$ while both values have uncertainties in the order of 10^{-3}. It is unlikely that the underestimation of the uncertainties of $\tilde{B}_1$ and $\tilde{B}_2$ discussed in section 2.1 can account for this because even if the errors in these values are increased by a factor of ten (hence making the values for $H^{35}Cl$ be in very good agreement with the published ones: see section 2.2.1) and propagated the uncertainties in k increase by only a little over a factor of ten. This gives the difference between the obtained values as over 500 standard deviations hence showing that this is very unlikely to be caused due to random errors.

Systematic errors are also unlikely to explain this difference as both values of k were obtained from data from the same spectrum and were calculated using differences in wavenumber values thus any constant systematic errors in the absorption wavenumber will have been removed and if any systematic errors were introduced in the data analysis they should be the same for both k values hence still making them comparable.

It is possible that the isotopic mass affects the value of k indirectly hence leading to the observed differences as previously found by Biernacki and Clerjaud for the SiH_4 and SiD_4 isotopologues.[4] However to more confidently confirm this more data with a lower random error in the data derived from the overtone transition should be obtained (as discussed in section 2.1). Additionally the rotational-vibrational spectrum of deuterated HCl gas could be recorded which should have an even greater value of k since the reduced mass is around a factor of two greater.

References

(1) K. Huber and G. Herzberg, *Constants of Diatomic Molecules*, ed. P. Linstrom and W. Mallard, (data prepared by J.W. Gallagher and R.D. Johnson, III) in NIST Chemistry WebBook, NIST Standard Reference Database Number 69, `https://doi.org/10.18434/T4D303` (visited on 04/12/2018).

(2) I. G. Hughes and T. P. A. Hase, *Measurements and their Uncertainties*, Oxford University Press, Oxford, 2010.

(3) *CRC Handbook of Chemistry and Physics*, ed. W. M. Haynes, CRC Press, Boca Raton, 97th edn., 2016.

(4) S. W. Biernacki and B. Clerjaud, *Physical Review B*, 2001, **63**, 075201-1 –075201-6.

3 Supplementary Information

3.1 Centrifugal Distortion Coefficients

The values of the centrifugal distortion coefficients, $\tilde{D_\nu}$, were determined from the gradients determined in the linear regressions.

Table 6: Centrifugal distortion coefficients.

	ν	$\tilde{D_\nu}$ / 10^{-4} cm^{-1}
^{35}Cl	0	5.25 ± 0.04
	1	5.11 ± 0.02
	2	4.3 ± 0.8
^{37}Cl	0	5.20 ± 0.03
	1	5.13 ± 0.01
	2	11 ± 4

3.2 Derivation of Vibrational Constant Equations

The energies associated with the discrete vibrational energy levels in a molecule are given by equation 3.2.1 which can be found through the application of perturbation theory on the harmonic potential with the perturbation of the potential including terms a of higher order than two from the Taylor expansion of the potential energy.

$$\tilde{E_\nu} = \tilde{\nu_e}\left(\nu + \frac{1}{2}\right) - \tilde{\nu_e}x_e\left(\nu + \frac{1}{2}\right)^2 \tag{3.2.1}$$

From equation 3.2.1 we can obtain the energy related to the pure vibrational transition $\tilde{E}(\nu_f \leftarrow 0)$ (the $\nu = 0$ to $\nu = \nu_f$ transition) as equation 3.2.2.

$$\begin{aligned}\tilde{E}\left(\nu_f \leftarrow 0\right) &= \tilde{E}_{\nu_f} - \tilde{E}_0 \\ &= \tilde{\nu_e}\left(\nu_f + \frac{1}{2} - \frac{1}{2}\right) - \tilde{\nu_e}x_e\left(\frac{1}{4} - \left(\nu_f + \frac{1}{2}\right)^2\right) \\ &= \tilde{\nu_e}\left(\nu_f - \left(\nu_f^2 + \nu_f\right)x_e\right)\end{aligned} \tag{3.2.2}$$

The energy related to the R branch transitions can be determined to yield equation 3.2.3 where J is the rotational state adopted in the lower vibrational state ($\nu = 0$).

$$R(J) = \Delta\tilde{E}(\nu_f \leftarrow 0) + (\tilde{B_{\nu_f}} + \tilde{B_0})(J+1) + (\tilde{B_{\nu_f}} - \tilde{B_0})(J+1)^2 \tag{3.2.3}$$

Setting $J = 0$ hence gives equation 3.2.4.

$$R(J) - 2\tilde{B_{\nu_f}} = \Delta\tilde{E}(\nu_f \leftarrow 0) \tag{3.2.4}$$

Substituting equation 3.2.2 into equation 3.2.4 yields equation 3.2.5.

$$R(0) - 2\tilde{B_{\nu_f}} = \tilde{\nu_e}\left(\nu_f - \left(\nu_f^2 + \nu_f\right)x_e\right) \tag{3.2.5}$$

Now from equation 3.2.5 a system of linear equations can be obtained by setting $\nu_f = 1$ and $\nu_f = 2$ (equations 3.2.6 and 3.2.7).

$$R(0) - 2\tilde{B_1} = \tilde{\nu_e}\left(1 - 2x_e\right) \tag{3.2.6}$$

$$R(0) - 2\tilde{B_2} = \tilde{\nu_e}\left(1 - 6x_e\right) \tag{3.2.7}$$

Solving equations 3.2.6 and 3.2.7 for $\tilde{\nu_e}$ and x_e then gives equations 1.3.1 and 1.3.2.